J. Biochem. **144,** 77–85 (2008)
doi:10.1093/jb/mvn041

Investigating a Catalytic Mechanism of Hyperthermophilic L-Threonine Dehydrogenase from *Pyrococcus horikoshii*

Noriko Higashi[1], Koichi Tanimoto[1], Motomu Nishioka[1], Kazuhiko Ishikawa[2] and Masahito Taya[1,*]

[1]Graduate School of Engineering Science, Osaka University, 1-3 Machikaneyama-cho, Toyonaka, Osaka 560-8531; and [2]National Institute of Advanced Industrial Science and Technology (AIST), 1-8-31 Midorigaoka, Ikeda, Osaka 563-8577, Japan

Received October 28, 2007; accepted March 15, 2008; published online April 4, 2008

Based on our first structural data of L-threonine dehydrogenase (TDH) of *Pyrococcus horikoshii* (PhTDH), we examined its catalytic mechanism. The structural analysis indicated that a catalytic zinc atom at the active centre of PhTDH is coordinated by four residues (Cys42, His67, Glu68 and Glu152) with low affinity. These residues are highly conserved in alcohol dehydrogenases (ADHs) and TDHs. Several PhTDH mutants were prepared with respect to Glu152 and other residues, relating to the proton relay system that is substantially a rate-limiting step in ADH. It was found that the E152D mutant showed 3-fold higher turnover rate and reduced affinities toward L-threonine and NAD^+, compared to wild-type PhTDH. The kinetic analysis of Glu152 mutants indicated that the carboxyl group of Glu152 is important for expressing the catalytic activity. The results obtained from pH dependency of kinetic parameters suggested that Glu152 to Asp substitution causes the enhancement of deprotonation of His47 or ionization of zinc-bound water and threonine in the enzyme-NAD^+ complex. Furthermore, it was predicted that the access of threonine substrate to the enzyme-NAD^+ complex induces a large conformational change in the active domain of PhTDH. From these results, we propose here that the proton relay system works as a catalytic mechanism of PhTDH.

Key words: activity-enhanced mutant, archaea, enzymatic kinetics, proton relay mechanism, site-directed mutagenesis.

Abbreviations: ADH, alcohol dehydrogenase; HlADH, horse liver ADH; OE-PCR, overlap extension PCR; PhTDH, *Pyrococcus horikoshii* TDH; Ss ADH, *Sulfolobus solfataricus* ADH; TDH, threonine dehydrogenase.

A hyperthermophilic anaerobic archaeon, *Pyrococcus horikoshii*, was isolated from a hydrothermal volcanic vent in the Okinawa Trough in the Pacific Ocean (*1*). From the genome database of *P. horikoshii* (*2*), we cloned a gene (PH0655) and the recombinant enzyme over-expressed in *Escherichia coli* was characterized as a hyperthermophilic L-threonine dehydrogenase (TDH) (*3*). TDH from *P. horikoshii* (PhTDH) could catalyse the oxidation of L-threonine to 2-amino-3-oxobutanoate. Our previous study reported that PhTDH exhibited substrate specificity for secondary alcohols with a high affinity to L-threonine and NAD^+. As PhTDH has broad substrate specificity, the enzyme is expected to be used for the synthesis of some chiral compounds. The PhTDH structure was a tetramer and the molecule composed of two dimers of 37.8 kDa. PhTDH was classified as a member of medium-chain, NAD(H)-dependent, and zinc-containing alcohol/polyol dehydrogenase family.

Based on the crystal structure of PhTDH, the analyses of enzymological similarities between TDH and alcohol dehydrogenase (ADH) will extend the biological knowledge concerning these enzymes. Some studies reported the relationship between structures and catalytic mechanisms of various ADHs (*4–6*). Mutational analyses of active sites in ADHs and TDHs have been also carried out to clarify the roles of amino acid residues in the enzymatic reactions (*4*, *7–9*).

Plapp and co-workers (*4*) proposed a proton relay system as the catalytic mechanism of horse liver ADH (HlADH) by mutagenesis of key amino acid residues and kinetic analyses of the enzymatic activities, on the basis of coenzyme-binding crystal structure model (PDB entry code: 1QLH). Moreover, they explained the substrate and coenzyme binding with a conformational change in HlADH, based on an induced fit mechanism using an extended ternary complex model (*10*).

ADH and TDH are generally assigned to the zinc-containing metalloenzymes. In the case of ADHs which contain two zinc atoms in one molecule, *i.e.* structural and catalytic ones, the amino acid residues participating in the metal coordination have been identified as the ligands (*5*, *6*). In the case of TDHs, however, there are few reports dealing with the residues for the metal ligands. Recently, we first succeeded in solving the crystal structure of PhTDH (*11*, *12*). PhTDH contained only one structural zinc atom coordinated to four cysteine residues (Cys97, Cys100, Cys103 and Cys111) per its subunit. Moreover, four residues associated with zinc atom in an ADH catalytic domain were also conserved

*To whom correspondence should be addressed. Tel: +81-6-6850-6251, Fax: +81-6-6850-6254,
E-mail: taya@cheng.es.osaka-u.ac.jp

in PhTDH. In ADH, the corresponding residues are Cys42, His67, Glu68 and Glu152, and the former three residues are identified to be catalytic zinc ligands. However, catalytic zinc atom was not observed in the crystal of PhTDH. Consequently the catalytic triad residues among these four residues are not yet identified in PhTDH.

In the present study, based on our structural data, we conduct the site-directed mutagenesis to investigate the catalytic domain and reaction mechanism of PhTDH. Especially, our interest is paid to the mutant enzyme obtained by substitution of Glu152 to Asp in the catalytic domain, because of its enhanced activity over wild-type PhTDH. From the kinetic analysis for wild-type PhTDH and E152D mutant, we here propose that the proton relay mechanism functions in PhTDH catalytic reaction.

EXPERIMENTAL PROCEDURES

Site-Directed Mutagenesis—The gene encoding PhTDH (ORF: PH0655) was cloned into *E. coli* JM109 using a pET-11a expression vector (Novagen, WI, USA), as described elsewhere (*3*). Site-directed mutagenesis was performed by the overlap extension PCR (OE-PCR) method (*13*), employing wild-type PhTDH gene as a template together with a set of mutagenic primers containing the designed mutations. All PCRs were carried out by using KOD-Plus DNA polymerase (Toyobo, Osaka, Japan), according to a conventional procedure. The sequences of the genes were verified by DNA sequencing using an ABI PRISM 310 genetic analyzer (Applied Bio-Systems, CA, USA).

Expression and Purification of Wild-Type and Mutant PhTDH Proteins—Wild-type PhTDH and its mutants were expressed in *E. coli* BL21 (DE3) and purified to homogeneity according to the procedures described elsewhere (*3*). The transformed cells overexpressing wild-type and mutant PhTDH proteins were cultivated in LB medium containing 0.05 mg/ml ampicillin. At prescribed culture time, the recombinant proteins were induced by adding 1 mM isopropyl β-D-thiogalactopyranoside to the cultures, followed by further culturing for 6 h. The cultured cells were collected by centrifugation and the crude proteins were extracted from the cells by means of ultrasonication in 50 mM Tris (2-amino-2-hydroxymethyl-1, 3-propanediol)-HCl buffer (pH 8.0). The extract was incubated at 85°C for 30 min and then centrifuged at 8,000*g* for 20 min to remove precipitants. The supernatant was dialysed against 50 mM Tris–HCl buffer (pH 8.0), and then purified on HiTrap Q and HiTrap Phenyl HP columns (GE Healthcare, Bucks, UK). The purity of pooled fractions for wild-type and mutant PhTDH proteins was confirmed as a single band on sodium dodecylsulphate-polyacrylamide gel electrophoresis (SDS–PAGE).

Each of the purified mutant proteins had a molecular mass of ~38 kDa on SDS–PAGE, being in agreement with the calculated molecular mass of 37.8 kDa for wild-type PhTDH. The protein concentration was determined with a Coomassie protein assay reagent (Pierce Chemical Company, IL, USA), using bovine serum albumin as a standard.

Kinetic Analysis—Enzyme activity was determined as described previously (*3*). The data of initial reaction rate were collected at 65°C with a V-550 spectrophotometer equipped with a Peltier ETC-505T temperature controller (Jasco, Tokyo, Japan). The assay mixture contained L-threonine and NAD^+ as a substrate and coenzyme, respectively, in 25 mM sodium phosphate buffer at pH 7.5. According to necessity, the concentrations of substrate and coenzyme were changed ranging from 0.2 to 20 times those of respective Michaelis constant values.

The mixture was pre-incubated for 5 min at 65°C in a quartz cuvette before the reaction was initiated by addition of the enzyme to the mixture. The time profile of NADH formation was monitored by measuring an increase in absorbance at 340 nm by spectrophotometry (*7*). One unit of enzyme activity represented the amount of enzyme producing 1 μmol of NADH per minute, which was calculated employing an absorption coefficient of $6.22\,mM^{-1}\,cm^{-1}$ for NADH at 340 nm. A blank test was conducted under each condition in the absence of the enzyme. The data were analysed by a non-linear regression fitting to the Michaelis–Menten equation.

The pH dependencies of kinetic parameters for wild-type PhTDH and selected mutant were determined at 65°C in Ellis and Morrison buffer (*14*) consisting of three components, 25 mM acetic acid, 25 mM MES (2-morpholin-4-ylethanesulfonic acid) and 50 mM Tris, the pH value of which was changed from 5 to 11 with 1 M HCl or NaOH. The conditions for the enzyme reaction under the different pHs were the same as mentioned previously, except for the buffer system.

Model Construction of PhTDH Active Domain—A structural model of PhTDH active domain was based on the 2.05 Å resolution crystal structure of enzyme-NAD^+ complex (PDB entry code: 2DFV) (*12*). The coordinates of amino acid residues and associations with related molecules were prepared using software MOLSCRIPT (*15*).

RESULTS

Active Site of PhTDH—The medium-chain NAD(H)-dependent ADHs, most of which have two zinc atoms per their subunit, are widely distributed in organisms (*5*, *6*, *16*). A high degree of conservation in some amino acid sequences is found in the medium-chain ADHs and TDHs, especially in their active sites. In our previous study (*3*), it was reported that PhTDH contains 1.22 ± 0.02 mol of zinc atom per mole of subunit protein based on inductively coupled plasma atomic emission spectroscopy, and it was also demonstrated that the zinc atom contributes to PhTDH thermostability examined by differential scanning calorimetry. From the structure of PhTDH, moreover, it was found that this zinc atom is coordinated with four cysteine residues (Cys97, Cys100, Cys103 and Cys111), holding an ideal tetrahedral geometry, as similarly observed in HlADH (*17*).

Four amino acid residues associated with catalytic zinc atom are also conserved in several TDHs and ADHs, as presented in Tables 1 and 2, respectively (*12*). Meanwhile, the active site of apo-*Sulfolobus solfataricus* ADH (SsADH) composes of one zinc atom and four amino acid residues (Cys38, His68, Glu69 and Cys154) which are conserved among TDHs and ADHs (*5*, *12*). The corresponding residues in PhTDH are Cys42, His67,

Table 1. **Alignments of amino acid residues of TDHs from selected origins.**

Source organisms				
Pyrococcus horikoshii	35	KVLATSICGTDLHIYEWNEWAQSRIKPPQIMGHEVA	133	IWKNPKSIPPEYATLQEPLGNAVDTVLAGP-ISGKSVLI
Pyrococcus abyssi	35	KVIATSICGTDLHIYEWNEWAQSRIKPPQIMGHEVA	133	VWKNPKSIPPEYATLQEPLGNAVDTVLAGP-ISGKSVLI
Pyrococcus furiosus	35	KILATSICGTDLHIYEWNEWAQTRIRPPQIMGHEVA	133	VWKNPKNIPPEYATLQEPLGNAVDTVLAGP-IAGKSVLI
Thermococcus kodakaraensis	35	KVLATSICGTDLHIYEWNEWAQSRIKPPQIMGHEVA	133	AWKNPKDMPPEYAALQEPLGNAVDTVLAGP-IAGRSTLI
Thermus thermophilus	31	RVEAASICGTDLHIWKWDAWARGRIRPPLVTGHEFS	129	AWVNPKDLPFEVAAILEPFGNAVHTVYAGSGVSGKSVLI
Bacillus subtilis	36	KVKAASICGTDVHIYNWDQWARQRIKTPYVFGHEFS	134	IWRNPADMDPSIASIQEPLGNAVHTVLESQ-PAGGTTAV
Escherichia coli	31	KIRKTAICGTDVHIYNWDEWSQKTIPVPMVVGHEYV	129	AFKIPDNISDDLAAIFDPFGNAVHTALSFD-LVGEDVLV
Xanthomonas campestris	31	KLEKTAICGTDLHIYLWDEWSQRTITPGLTIGHEFV	129	LWPIPDQIPSELAAFFDPYGNAAHCALEFD-VIGEDVLI
		***** ** * * * ***		* * * **** *

The identical amino acid residues among these eight proteins are shown by the asterisks. The underlined letters indicate the conserved residues as a catalytic site among TDHs.

Table 2. **Conserved amino acid residues associated with proton transfer in TDH and ADHs from selected origins.**

Enzymes				
Pyrococcus horikoshii TDH	35	KVLATSI*C*GTDLHIYEWNEW-----AQSRIKPPQIMG*HE*VA	146	EYATLQEPLGNAV
Aeropyrum pernix ADH	47	RIAGAGV*C*HTDLHLVQGMWH-----ELLQPKLPYTLG*H*ENV	162	EMAPLA*D*AGITAY
Sulfolobus solfataricus ADH	31	KVEAAGV*C*HSDVHMRQGRFGNLRIVEDLGVKLPVTLG*H*EIA	148	EAAPLT*C*SGITTY
Horse liver ADH	39	KMVATGI*C*RSDDHVVSG---------TLVTPLPVIAG*H*EAA	168	KVCLIG*C*GFSTGY

The italic and underlined letters indicate the putative zinc ligands and conserved residues associated with proton transfer, respectively. The gaps introduced for optimum alignment are indicated by dashed lines, and the numerals represent the position of the first residue in each sequence.

Glu68 and Glu152 (Table 2). However, the catalytic zinc atom was not recognized in the crystal of PhTDH. When PhTDH was treated with EDTA and then soaked in nickel chloride solution, the electron density of nickel atom was observed in crystallized PhTDH. Moreover, it was observed that the addition of Zn^{2+} (0.01–1.0 mM) to the reaction mixture caused the enhancement of PhTDH activity (data not shown). These results support the possible coordination of catalytic zinc atom to Cys42, His67 and Glu68 identified as an active site in the crystal of PhTDH, as illustrated in Fig. 1A. The combination among Cys42, His67 and Glu68 in PhTDH seems to be different from that in ADHs, as predicted in the previous report (*12*). In the present work, we particularly focus on the role of Glu152 residue because this residue is expected to be involved in the catalytic function in an indirect manner.

Alternative residues important for the ADH activity are Ser48 and His51, which are involved in the proton relay mechanism in HlADH (*4*). In the case of PhTDH, the corresponding residues are Thr44 and His47, which are also conserved in the other TDHs (Table 1). The structural model of PhTDH revealed that Thr44 and His47 located at 6.54 and 5.74 Å, respectively, from the 2′-hydroxyl group of nicotinamide ribose of NAD(H) (Fig. 1B), and that the distances were somewhat far as compared with those observed in HlADH (Fig. 1C). The resemblance of amino acid residues in the active sites between ADHs and TDHs strongly suggests that a similar mechanism works in their catalytic reactions. In the present study, a proton relay mechanism in PhTDH catalysis is proposed, as illustrated in Scheme 1, in analogy with HlADH. In the case of ADH, the hydroxyl group of conserved Ser or Thr residue is known to play an important role in forming a hydrogen bond with zinc-bound water molecule or substrate in the proton relay system (Table 2) (*4*, *5*, *18*, *19*). In PhTDH, the conserved residue Thr44 can be responsible for functioning as the corresponding part in the proton relay mechanism. In the present work, as shown in Table 3, it was found that the mutation of Thr44 to Ala in PhTDH completely lost its activity, supporting that the proposed scheme is reasonable, in accordance with the prediction in the structural study of PhTDH (*12*).

Kinetic Properties—To know the effect of ionization of amino acid residues on the catalytic activity of PhTDH, the pH dependence of kinetic parameters was examined in terms of turnover rate constant (k_{cat}) and Michaelis constant for L-threonine (K_{m-T}). The plots of logk_{cat} and log(k_{cat}/K_{m-T}) versus pH for wild-type PhTDH are shown in Fig. 2A and B, respectively. The relation between logk_{cat} and pH exhibited an apparent slope of less than unity, which suggests that the group concerning the rate-limiting step is not a single ionizable residue. It is thus considered that at least two different ionizable groups are responsible for inducing the maximal activity of PhTDH. Through some trials, in the present study, the proton dissociation model with two catalytic forms among three ionizable groups was derived to explain the experimental data in the examined pH region,

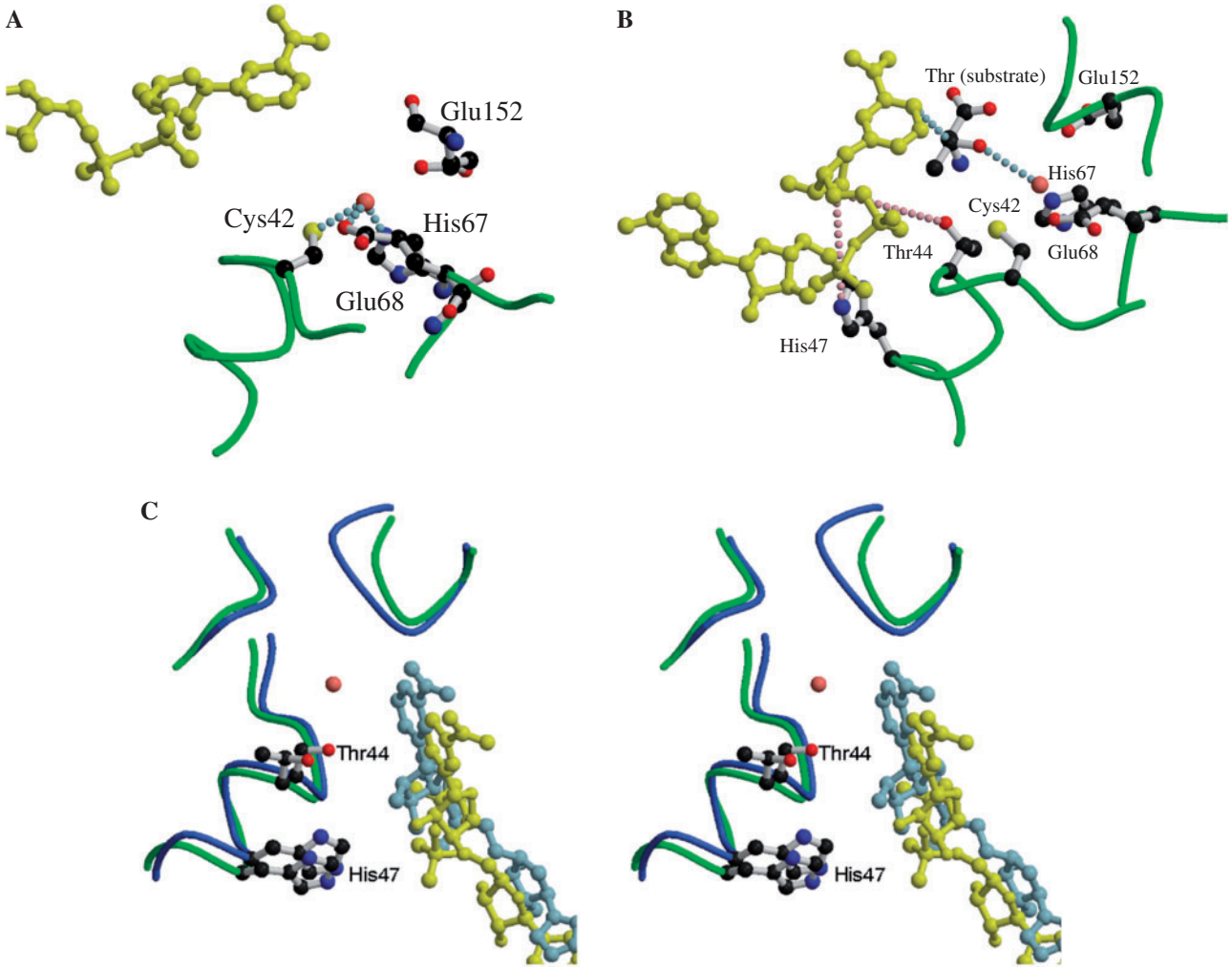

Fig. 1. **Structure of active domain in binary complex of PhTDH and NAD$^+$.** (A) Active site showing catalytic zinc ligands. The catalytic zinc atom is shown in a pink sphere. The NAD$^+$ molecule is shown by a yellow ball and stick model. The dashed blue lines present zinc coordinate bonds. The backbone trace is indicated in green wires with some highlighted residues shown by a coloured ball and stick model. (B) Active site showing coordination in proton transfer system. L-Threonine as a substrate is placed at the speculated position between active zinc atom (pink) and C4 position of nicotinamide ring of NAD$^+$ (yellow). Putative interactions are indicated by the dashed lines. (C) Stereoscopic view of superimposed C$^\alpha$ traces of NAD(H)-binding domains in PhTDH (green) and NAD$^+$ (yellow) complex and double mutant HlADH (blue) and NAD$^+$ (light blue) complex (PDB entry code: 1QLH). The catalytic zinc atom is shown in a pink sphere.

as illustrated in Scheme 2. The model represents the participation of four species of ternary complex, $EH_1H_2H_3$·S-NAD$^+$, EH_2H_3·S-NAD$^+$ (EH_1H_3·S-NAD$^+$), EH_3·S-NAD$^+$ and E·S-NAD$^+$ (catalytic forms of interest: EH_2H_3·S-NAD$^+$ and EH_3·S-NAD$^+$), while considering three ionizable groups.

The protons, H_1, H_2 and H_3, dissociate in turn with an increase in pH value and the dissociations of these three protons are independent without interactions with each other. According to Scheme 2, the dissociation constants of concerned complexes are defined as follows (*20*, *21*).

$$K_a = \frac{[H^+][EH_2H_3 - NAD^+]}{[EH_1H_2H_3 - NAD^+]} = \frac{[H^+][EH_3 - NAD^+]}{[H_1H_3E - NAD^+]} \quad (1)$$

$$K_b = \frac{[H^+][EH_1H_3 - NAD^+]}{[EH_1H_2H_3 - NAD^+]} = \frac{[H^+][EH_3 - NAD^+]}{[EH_2H_3 - NAD^+]} \quad (2)$$

$$K_{aS} = \frac{[H^+][EH_2H_3 \cdot S - NAD^+]}{[EH_1H_2H_3 \cdot S - NAD^+]} = \frac{[H^+][EH_3 \cdot S - NAD^+]}{[EH_1H_3 \cdot S - NAD^+]} \quad (3)$$

$$K_{bS} = \frac{[H^+][EH_1H_3 \cdot S - NAD^+]}{[EH_1H_2H_3 \cdot S - NAD^+]} = \frac{[H^+][EH_3 \cdot S - NAD^+]}{[EH_2H_3 \cdot S - NAD^+]} \quad (4)$$

$$K_{s1} = \frac{[S][EH_2H_3 - NAD^+]}{[EH_2H_3 \cdot S - NAD^+]}, \quad K_{s2} = \frac{[S][EH_3 - NAD^+]}{[EH_3 \cdot S - NAD^+]} \quad (5)$$

Here, K_a and K_{aS} are dissociation constants for proton H_1, and K_b and K_{bS} are those for proton H_2. K_{s1} and K_{s2} are dissociation constants for enzyme-substrate complexes. In the present study, the deprotonation of complexes in terms of K_c and K_{cS} are not considered owing to the experimental limitation under an extremely high pH condition. Based on Eqs. 2–5, k_{cat} and k_{cat}/K_{m-T}

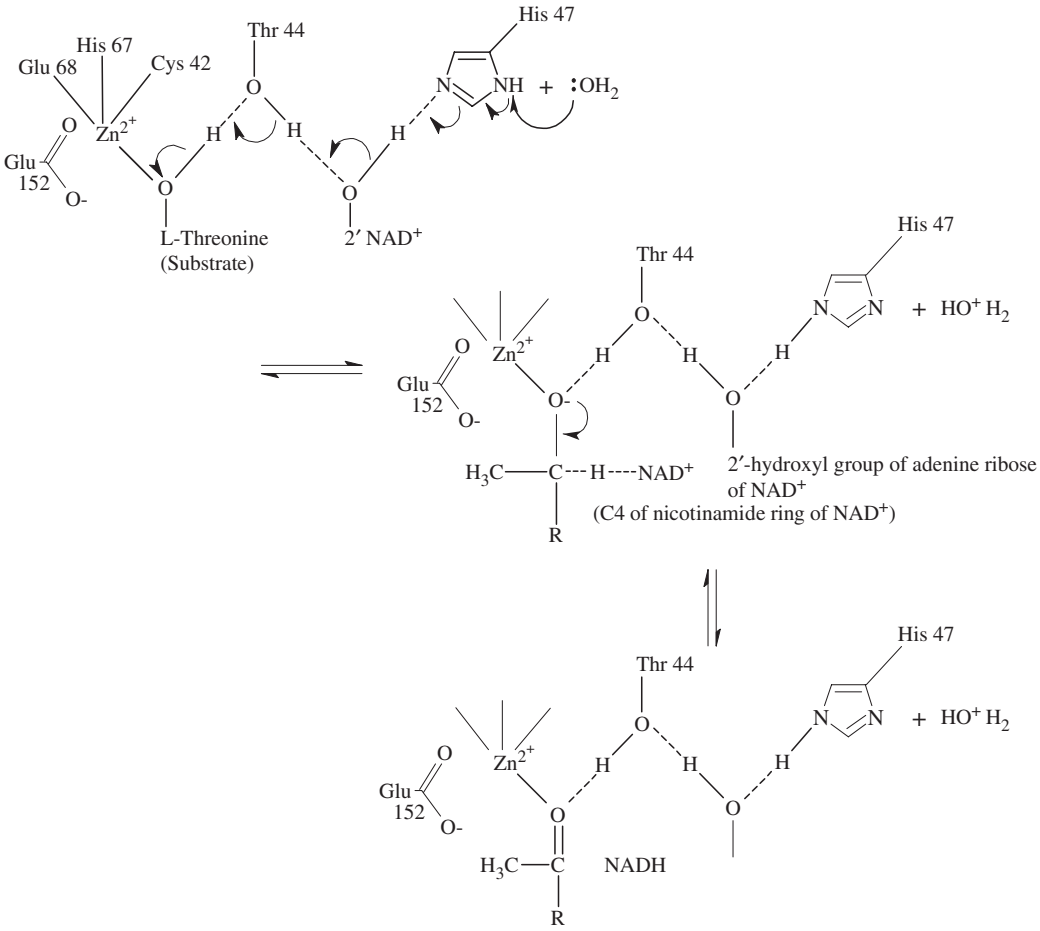

Scheme 1. **Possible mechanism of proton relay system in PhTDH.**

are given by the following equations as a function of hydrogen ion concentration.

$$k_{cat} = \frac{k_1 K_{aS}[H^+] + k_2 K_{aS} K_{bS}}{[H^+]^2 + (K_{aS} + K_{bS})[H^+] + K_{aS} K_{bS}} \quad (6)$$

$$\frac{k_{cat}}{K_{m-T}} = \frac{k_1/K_{S1} \cdot K_{aS}[H^+] + k_2/K_{S2} \cdot K_{aS} K_{bS}}{[H^+]^2 + (K_a + K_b)[H^+] + K_a K_b} \quad (7)$$

where k_1 and k_2 are reaction rate constants at the rate-limiting steps forming product, P, from $EH_2H_3{\cdot}S{-}NAD^+$ and $EH_3{\cdot}S{-}NAD^+$, respectively.

As depicted by the solid lines in Fig. 2, the pH profiles of logk_{cat} and log (k_{cat}/K_{m-T}) were calculated by fitting Eqs. 6 and 7 to the data for wild-type PhTDH using a non-linear least-squares regression algorithm (*17*, *20*). It is seen that the calculated lines follow the experimental data in fair agreement. Table 4 lists the determined values of kinetic parameters and dissociation constants for wild-type PhTDH. The pK_{aS} and pK_{bS} values were estimated to be 6.28 and 7.76, respectively, with respect to two ionizable groups in the enzyme. The k_2 value was larger than the k_1 value, indicating that the complex form, $EH_3 \cdot S - NAD^+$, can make relatively large contribution to the enzyme activity.

Mutation Analyses—The Glu residue at the position 152 in PhTDH is included in the proton relay system according to its crystal data, but it forms hydrogen and/or ionic bonds near the electron transfer site of NAD(H) together with Glu92, His94 and Arg294 (*12*). In order to understand the role of Glu152 in the catalytic mechanism, we prepared several PhTDH mutants with respect to Glu152 using the site-directed mutagenesis. The kinetic parameters for wild-type PhTDH and its Glu152 mutants are presented in Table 3. The enzyme activities of mutants E152Q, E152A and E152K disappeared almost completely and the other mutants retained their activities to some extent (see maximum reaction rate V_m in Table 3). It is worth noting that k_{cat} of mutant E152D is 3-fold higher than that of the wild-type enzyme. In addition, E152D displayed 20- and 40-fold increases in K_m for L-threonine and NAD^+, respectively, and exhibited a 6-fold decrease in k_{cat}/K_{m-T} compared to wild-type PhTDH, supporting the view that Glu152 makes contribution to substrate binding to the enzyme.

In order to know why E152D mutant showed 3-fold higher k_{cat} over the wild-type enzyme, the pH dependence of kinetic parameters was examined with respect to this mutant enzyme. Figure 2 also shows the plots

Table 3. **Kinetic parameters of wild-type PhTDH and its mutants.**

Enzyme	V_m (U mg^{-1})	K_{m-T} (mM)	K_{m-NAD+} (mM)	k_{cat} (min^{-1})	k_{cat}/K_{m-T} (mM^{-1}min^{-1})
Wild-type	1.76 ± 0.03	0.0118 ± 0.0023	0.0099 ± 0.0012	66.5 ± 1.0	5640 ± 1110
E152D	5.58 ± 0.36	0.237 ± 0.019	0.399 ± 0.035	210 ± 14	886 ± 90
E152C	0.385 ± 0.075	0.308 ± 0.037	0.163 ± 0.048	14.5 ± 2.8	47.2 ± 10.8
E152Q	0.0163 ± 0.0042	50.6 ± 8.8	0.216 ± 0.111	0.617 ± 0.158	0.0122 ± 0.0038
E152S	0.135 ± 0.037	21.2 ± 3.2	0.607 ± 0.162	5.10 ± 1.16	0.241 ± 0.066
E152A	0.0145 ± 0.001	17.5 ± 0.9	0.0615 ± 0.0357	0.547 ± 0.303	0.0313 ± 0.0024
E152T	0.127 ± 0.005	23.6 ± 4.3	0.152 ± 0.017	4.81 ± 0.170	0.204 ± 0.038
E152K	ND	–	–	–	–
T44A	ND	–	–	–	–
R294A	0.205 ± 0.003	5.32 ± 1.48	0.105 ± 0.009	7.76 ± 0.12	1.46 ± 0.41

ND: Not detected. –: Not determined.

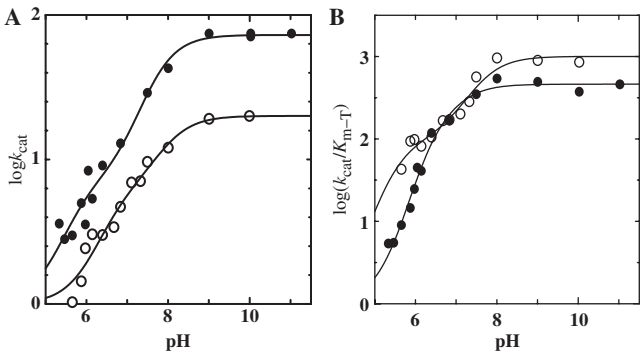

Fig. 2. **pH dependencies of kinetics parameters of wild-type PhTDH and E152D mutant**. (A) Plots of logk_{cat} against pH. (B) Plots of log(k_{cat}/K_{m-T}) against pH. The solid lines represent the best fits of Eqs. 6 and 7 to the experimental data.

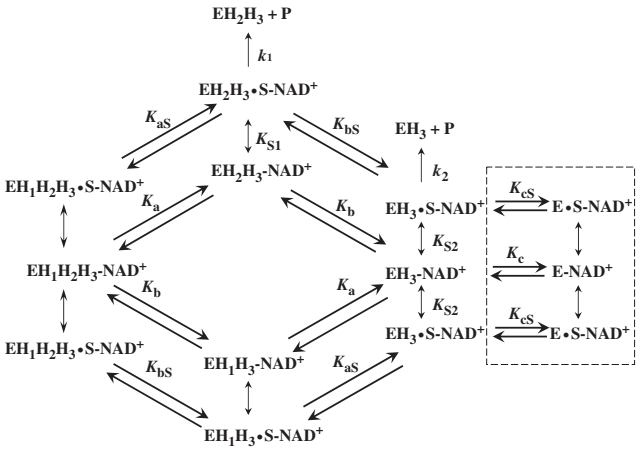

Scheme 2. **Proton dissociation model for PhTDH. The dissociations in the dashed line box are not included in deriving Eqs. 6 and 7.**

of logk_{cat} and log(k_{cat}/K_{m-T}) against pH as well as the fitting results with respect to E152D. The substitution of Glu152 to Asp, as listed in Table 4, caused acidic shifts of the pK_{aS} and pK_{bS} values from 6.28 to 5.41 and from 7.76 to 7.32, respectively. Compared to the wild-type enzyme, in addition, the k_1 and k_2 values changed from 0.825 to 0.879 min^{-1} and from 1.30 to 1.86 min^{-1}, respectively, indicating that the mutation exerted a relatively large effect on the k_2 value.

Table 4. **Dissociation constants and kinetic parameters estimated from pH dependences for wild-type PhTDH and E152D mutant.**

	Wild-type	E152D
pK_a	4.90 ± 0.30	5.82 ± 0.14
pK_b	7.26 ± 0.20	6.97 ± 1.47
pK_{aS}	6.28 ± 0.23	5.41 ± 0.22
pK_{bS}	7.76 ± 0.54	7.32 ± 0.21
k_1 (min^{-1})	0.825 ± 0.212	0.879 ± 0.139
k_2 (min^{-1})	1.30 ± 0.07	1.86 ± 0.05
K_{S1} (mM)	0.410 ± 0.110	0.365 ± 0.087
K_{S2} (mM)	0.433 ± 0.025	0.699 ± 0.023

From a different aspect, we attempted to introduce an additional zinc atom into the active site to improve the activity of PhTDH by substitution at Glu152, based on the information on SsADH with high homology to PhTDH (*22*) (Table 2). In SsADH, the corresponding residue to PhTDH Glu152 is Cys154, and this residue is a zinc ligand. The Cys substitution at Glu152 (E152C) in PhTDH resulted in a decrease in the catalytic activity (Table 3). As demonstrated in the previous paper (*12*), Arg294 located in the active site makes an electrostatic interaction with Glu152 in PhTDH. This consideration is supported by the fact that R294A mutant had the decreased activity (V_m = 0.205 U/mg) and lower affinities for L-threonine (K_{m-T} = 5.32 mM) and NAD$^+$ (K_{m-NAD^+} = 0.105 mM) (Table 3).

DISCUSSION

Catalytic Zinc Atom and Ligands—PhTDH is the first TDH enzyme whose crystal structure was solved and the structure confirms an overall fold similar to that of ADH in spite of the relatively low sequence identity between these two dehydrogenases (*12*). Similarity in the crystal structures and kinetic properties between TDH and ADH enzymes strongly suggests the existence of quite analogical mechanism in their catalytic reactions.

PhTDH contains a structural zinc atom which is coordinated by four residues (Cys97, Cys100, Cys103

and Cys111) per subunit. These residues are conserved in several TDHs and ADHs (*12*). In the case of ADHs, additional zinc atom is assigned as the catalytic one (*5*, *6*) and is coordinated by three residues conserved in ADHs. In the crystal structure of PhTDH, the electron density of the catalytic zinc atom was not detected clearly at the active site. The activity of PhTDH was enhanced under the excess presence of zinc ions in the reaction mixture, suggesting that PhTDH requires alternative zinc coordinating to the active site for expressing the enzyme activity.

According to our previous study (*12*), PhTDH contains a catalytic zinc atom at the active centre coordinated by Cys42, His67, Glu68 and Glu152, but the zinc atom seems to be unstable at the site. We present the scheme of a possible proton relay system for the reaction mechanism of PhTDH (Scheme 1). The catalytic zinc atom is supported by a catalytic triad (Cys42, His67 and Glu68) and an ionizable zinc-bound water molecule bonded to the hydroxyl group of Thr44 in the active site. Catalytic zinc has a critical role to deprotonate the hydroxyl group of water or threonine substrate, and then the deprotonation process is involved in the proton transfer through several residues. In the case of HlADH, Ser48, His51 and NAD^+ are participating groups in the proton transfer system. Actually, when Thr44 in PhTDH, corresponding to Ser48 in HlADH, was replaced by alanine, the activity of PhTDH was completely lost (Table 3). This result justifies that the proton relay system is postulated to work in the catalytic reaction of PhTDH as shown in Scheme 1.

From the PhTDH crystal structural analysis, the zinc atom seems to be located at the bottom of a hydrophobic cleft and ligated by the aforementioned catalytic ligands (Cys42, His67 and Glu68) in the enzyme reaction (Fig. 1A), suggesting that the catalytic zinc atom at the active centre of PhTDH is coordinated by three residues (Cys42, His67 and Glu68) with weak interaction. This combination among three residues is different from ADHs (*8*) though four residues (Cys42, His67, Glu68 and Glu152) associated with catalytic zinc atom are highly conserved in ADHs and TDHs (Table 1 and 2) (*12*).

Catalytic Mechanism of PhTDH—In the oxidation of L-threonine, two hydrogen atoms are transferred, one atom as hydride ion being pulled out to the C4 position of the nicotinamide ring of NAD^+. The other hydrogen atom of the zinc-bound hydroxyl group of substrate is serially transferred to the hydroxyl group of Thr44, 2′-hydroxyl group position of adenine ribose of NAD^+ and His47, and released ultimately as proton. Such a route including the amino acid residues and functional groups is the proposed network as a proton transfer pathway observed in wild-type PhTDH. The correlation of relative positions of these participants is completely conserved in ADHs. But Thr44 in PhTDH is replaced by the corresponding residue Ser48 in HlADH, and its role in the proton relay system has been reported (*4*, *18*, *19*).

Generally, pH dependency of enzymatic activity reflects the ionization of groups involved in the catalysis. The parameters obtained from the steady-state kinetics can be correlated with the ionization of molecule(s) participating in the proton relay system. In the present work, the pH dependencies of wild-type PhTDH could be explained by the equations derived from the proton dissociation model (Scheme 2) where two of three proton dissociation steps were considered. Hence, the model equations were derived on the assumption that PhTDH reaction obeys the ordered Bi Bi mechanism, considering the fact that PhTDH crystal was gained in a state of enzyme-NAD^+ complex (*12*), together with the reports that this mechanism worked in the other TDH and ADH (*4*, *23*). Shimizu *et al*. (*24*) proposed that the oxidation reaction of L-threonine by PhTDH proceeds through the random mechanism. As they stated, however, an actual mechanism of whole PhTDH reaction process is not yet clear, because of experimental limitation arising from the unstable nature of a product, 2-amino-3-oxobutanoate. According to the presented model scheme, the estimated values of pK_a, pK_{aS}, pK_b and pK_{bS} (Table 4) may be assigned to the dissociation constants of histidine and hydroxyl group (*4*, *25–27*). Taking account of the key elements in the proton relay system of PhTDH, it may be reasonable to state that pK_a and pK_b are responsible for the deprotonation of His47 or catalytic zinc-bound water, and that pK_{aS} and pK_{bS} are for the deprotonation of His47 or zinc-bound threonine in the enzyme-NAD^+ complex (*28–30*).

Glu152 Mutants—In the proposed mechanism of PhTDH catalysis, as mentioned previously, the highly conserved residue Glu152 is not associated with the proton relay system and also does not participate directly in the coordination of zinc atom. However, it is likely that Glu152 residue stabilizes the catalytic zinc atom and oxygen atom of threonine in the enzyme reaction and controls the enzyme activity. Moreover, an electrostatic interaction of Glu152 with vicinal amino acid residues may not be negligible, being supported by the fact that the substitution at this residue exerted a significant effect on PhTDH catalysis.

Several mutants of Glu152 were constructed in this work and most of the mutants lost the activity or showed the reduced V_m values with an exception of E152D mutant. These results indicated that Glu152 engages in the rate-limiting step of the reaction in PhTDH. Considering the kinetic parameters of several Glu152 mutants, it is expected that a negatively charged carboxyl group is necessary in the vicinity of position Glu152 for expressing the enzyme activity. Also pH dependency of E152D mutant indicated that alteration in electrostatic environment, induced by shortening the negatively charged side-chain with carboxyl group, causes some changes in the proton relay system. As seen in Table 4, the substitution of Glu152 to Asp increased the k_2 value. For wild-type PhTDH, the pK_{aS} and pK_{bS} values were 6.28 and 7.76, and for E152D the pK_{aS} and pK_{bS} values were 5.41 and 7.32, respectively. These shifts of pK_{aS} and pK_{bS} toward the acidic values for the mutant are advantageous to facilitating the deprotonation of the concerned residues and molecules in the enzyme reaction under neutral to slightly alkaline conditions. In the reaction model of PhTDH presented here, the elevation of k_{cat} value is attributable to increases in the k_1 and k_2 values. When compared the

k_1 and k_2 values between wild-type PhTDH and E152D mutant, the change of k_1 value was relatively small and the increment in k_2 value seems to contribute to the enhancement of k_{cat} value for E152D mutant, being attributed from a stabilized transition state of the Michaelis complex and reduced activation energy in the rate-limiting step. These results suggest that the reaction pathway via the complex EH_3·S-NAD^+ (Scheme 2) is intensified by the substitution of Glu152 to Asp.

Glu152 and Arg294 forms hydrogen and/or ionic bonds near the electron transfer site of NAD(H) together with Glu92 and His94, and these residues are thought to be related to the substrate specificity (*12*), whereas the corresponding residue of Arg294 is not conserved in ADHs. Ala substitution at these residues may break the hydrogen or ionic bond between the relating residues and molecules. E152A and R294A mutants, however, showed the different tendencies in their activities. E152A mutant almost lost its activity whereas R294A mutant remained one-eighth activity of wild-type PhTDH with the larger K_{m-T} value, suggesting that both Arg294 and Glu152 are of importance for the binding of threonine substrate, in addition to Glu152 participation in the proton relay system. Arg294 residue may be essential for stabilizing the position of the carboxyl group of Glu152 important for the proton relay mechanism. The change in Glu152 side-chain caused by the mutation may also break an ionic bond to Arg294 side-chain, inducing changes in the active site structure and thereby in the catalytic activity. In addition, E152D mutant exhibited the increased V_m value with the large k_{cat} value, which is explained by the improved release of the product from the EH_2H_3·S–NAD^+ complex, as reflected in the improved k_2 value.

Conformational Change at Active Site—Based on the structural data of PhTDH-NAD^+ complex, the distance between the side-chain of Thr44 and 2′ position of adenine ribose of NAD^+ and that between oxygen atom of Thr44 and putative zinc position are 6.54 and 6.06 Å, respectively. In addition, His47, a member of the proton relay system, is 5.74 Å away from the 2′ position of adenine ribose of NAD^+ (Fig. 1B). These distances seem to be rather long for occurrence of proton transfer through a sequence of catalytic reaction, suggesting that a conformational change takes place when threonine substrate binds to PhTDH-NAD^+ complex, likewise predicted in ADH enzyme (*29*). In addition, the structural data indicates that Thr44 and His47 are located in the α1 helix with 6.54 and 5.74 Å distances from NAD^+ in the PhTDH-NAD^+ complex, whereas Ser48 and His51 are 2.83 and 4.81 Å away in the case of HlADH (Fig. 1C). Therefore it is supposed that the α1 helix moves towards the NAD^+ moiety when the substrate accesses to the binding site, just as explained by the induced fit mechanism of Koshland (*31*). According to this mechanism, the access of a bulky substrate to enzyme induces a large conformational change so that an active site is stabilized by electrostatic interaction in the α1 helix. In the case of PhTDH, it is most likely that the fragile binding of catalytic zinc atom makes it easier to induce such a conformational change in the active site.

In future work, thermodynamic studies will be undertaken for clarifying the mechanism of conformational change and its impact on the catalytic properties of both the wild-type and mutant enzymes.

The authors thank Emeritus Professor Noritake Yasuoka of Himeji Institute of Technology for his helpful advice to the present work. The authors also thank Dr Takanori Matsuura, Institute for Protein Research, Osaka University, for his support in operating the software MOLSCRIPT. This work was in part supported by the National Project on Protein Structural and Functional Analyses founded by the Ministry of Education, Culture, Sports, Science and Technology of Japan.

REFERENCES

1. Gonzalez, J.M., Masuchi, Y., Robb, F.T., Ammerman, J.W., Maeder, D.L., Yanagibayashi, M., Tamaoka, J., and Kato, C. (1998) *Pyrococcus horikoshii* sp. nov., a hyperthermophilic archaeon isolated from a hydrothermal vent at the Okinawa Trough. *Extremophiles* **2**, 123–130
2. Kawarabayasi, Y., Sawada, M., Horikawa, H., Haikawa, Y., Hino, Y., Yamamoto, S., Sekine, M., Baba, S., Kosugi, H., Hosoyama, A., Nagai, Y., Sakai, M., Ogura, K., Otsuka, R., Nakazawa, H., Takamiya, M., Ohfuku, Y., Funahashi, T., Tanaka, T., Kudoh, Y., Yamazaki, J., Kushida, N., Oguchi, A., Aoki, K., and Kikuchi, H. (1998) Complete sequence and gene organization of the genome of a hyperthermophilic archaebacterium, *Pyrococcus horikoshii* OT3. *DNA Res* **5**, 55–76
3. Higashi, N., Fukada, H., and Ishikawa, K. (2005) Kinetic study of thermostable L-threonine dehydrogenase from an archaeon *Pyrococcus horikoshii*. *J. Biosci. Bioeng.* **99**, 175–180
4. LeBrun, L.A., Park, D.H., Ramaswamy, S., and Plapp, B.V. (2004) Participation of histidine-51 in catalysis by horse liver alcohol dehydrogenase. *Biochemistry* **43**, 3014–3026
5. Esposito, L., Sica, F., Raia, C.A., Giordano, A., Rossi, M. Mazzarella, L., and Zagari, A. (2002) Crystal structure of the alcohol dehydrogenase from the hyperthermophilic archaeon *Sulfolobus solfataricus* at 1.85 Å resolution. *J. Mol. Biol.* **318**, 463–477
6. Guy, J.E., Isupov, M.N., and Littlechild, J.A. (2003) The structure of an alcohol dehydrogenase from the hyperthermophilic archaeon *Aeropyrum pernix*. *J. Mol. Biol.* **331**, 1041–1051
7. Epperly, B.R. and Dekker, E.E. (1991) L-Threonine dehydrogenase from *Escherichia coli*. Identification of an active site cysteine residue and metal ion studies. *J. Biol. Chem.* **266**, 6086–6092
8. Johnson, A.R., Chen, Y.W., and Dekker, E.E. (1998) Investigation of a catalytic zinc binding site in *Escherichia coli* L-threonine dehydrogenase by site-directed mutagenesis of cysteine-38. *Arch. Biochem. Biophys.* **358**, 211–221
9. Johnson, A.R. and Dekker, E.E. (1998) Site-directed mutagenesis of histidine-90 in Escherichia coli L-threonine dehydrogenase alters its substrate specifity. *Arch. Biochem. Biophys.* **351**, 8–16
10. Rubach, J.K. and Plapp, B.V. (2003) Amino acid residues in the nicotinamide binding site contribute to catalysis by horse liver alcohol dehydrogenase. *Biochemistry* **42**, 2907–2915
11. Higashi, N., Matsuura, T., Nakagawa, A., and Ishikawa, K. (2005) Crystallization and preliminary X-ray analysis of hyperthermophilic L-threonine dehydrogenase from archaeon. *Pyrococcus horikoshii, Acta Crystallograph. Sect. F Struct. Biol. Cryst. Commun.* **61**, 432–434
12. Ishikawa, K., Higashi, N., Nakamura, T., Matsuura, T., and Nakagawa, A. (2007) The first crystal structure of L-threonine dehydrogenase. *J. Mol. Biol.* **366**, 857–867

13. Ho, S.N., Hunt, H.D., Horton, R.M., Pullen, J.K., and Pease, L.R. (1989) Site-directed mutagenesis by overlap extension using the polymerase chain reaction. *Gene* **77**, 51–59
14. Ellis, K.J. and Morrison, J.F. (1982) Buffer of constant ionic strength for studying pH-dependent processes. *Methods Enzymol.* **87**, 405–426
15. Kraulis, P.J. (1991) MOLSCRIPT: a program to produce both detailed and schematic plots of protein structures. *J. Appl. Cryst.* **24**, 946–950
16. Esposito, L., Bruno, I., Sica, F., Raia, C.A., Giordano, A., Rossi, M. Mazzarella, L., and Zagari, A. (2003) Crystal structure of a ternary complex of the alcohol dehydrogenase from *Sulfolobus solfataricus*. *Biochemistry* **42**, 14397–14407
17. Eklund, H., Nordstrom, B., Zeppezauer, E., Soderlund, G., Ohlsson, I., and Boiwe, T. (1976) Three-dimensional structure of horse liver alcohol dehydrogenase at 2.4 Å resolution. *J. Mol. Biol.* **102**, 27–59
18. Ramaswamy, S., Park, D.H., and Plapp, B.V. (1999) Substitution in a flexible loop of horse liver alcohol dehydrogenase hinder the conformational change and unmask hydrogen transfer. *Biochemistry* **38**, 13951–13959
19. Eklund, H., Plapp, B.V., Samama, J.P., and Branden, C.I. (1982) Binding of substrate in a ternary complex of horse liver alcohol dehydrogenase. *J. Biol. Chem.* **257**, 14349–14358
20. Ishikawa, K., Matsui, I., Honda, K., Kobayashi, S., and Nakatani, H. (1991) The pH dependence of the action pattern in porcine pancreatic α-amylase-catalyzed reaction for maltooligosaccharide substrates. *Arch. Biochem. Biophys.* **289**, 124–129
21. Ishikawa, K., Matsui, I., Honda, K., Kobayashi, S., and Nakatani, H. (1990) Substrate-dependent shift of optimum pH in porcine pancreatic α-amylase-catalyzed reaction. *Biochemistry* **29**, 7119–7123
22. Watanabe, S., Kodaki, T., and Makino, K. (2005) Complete reversal of coenzyme specificity of xylitol dehydrogenase and increase of thermostability by the introduction of structural zinc. *J. Biol. Chem* **280**, 10340–10349
23. Aoyama, Y. and Motokawa, Y. (1981) L-Threonine dehydrogenase of chicken liver. Purification, characterization, and physiological significance. *J. Biol. Chem.* **256**, 12367–12373
24. Shimizu, Y., Sakuraba, H., Kawakami, R., Goda, S., Kawarabayasi, Y., and Ohshima, T. (2005) L-Threonine dehydrogenase from the hyperthermophilic archaeon *Pyrococcus horikoshii* OT3. *Extremophiles* **9**, 317–324
25. Kvassman, J. and Pettersson, G. (1978) Effect of pH on the process of ternary-complex interconversion in the liver-alcohol-dehydrogenase reaction. *Eur. J. Biochem.* **87**, 417–427
26. Anderson, P., Kvassman, J., Lindstrom, A., Olden, B., and Pettersson, G. (1981) Effect of NADH on the p*K*a of zinc-bound water in liver alcohol dehydrogenase. *Eur. J. Biochem.* **113**, 425–433
27. Pettersson, G. (1987) Liver alcohol dehydrogenase. *CRC Crit. Rev. Biochem.* **21**, 349–389
28. Eklund, H., Plapp, B.V., Samama, J.P., and Branden, C.I. (1982) Binding of substrate in a ternary complex of horse liver alcohol dehydrogenase. *J. Biol. Chem.* **257**, 14349–14358
29. Leskovac, V., Trivic, S., and Anderson, B.M. (1998) Use of competitive dead-end inhibitors to determine the chemical mechanism of action of yeast alcohol dehydrogenase. *Mol. Cell. Biochem.* **178**, 219–227
30. LeBrun, L.A. and Plapp, B.V. (1999) Control of coenzyme binding to horse liver alcohol dehydrogenase. *Biochemistry* **38**, 12387–12393
31. Koshland, D.E. (1958) Application of theory of enzyme specificity to protein synthesis. *Proc. Natl. Acad. Sci. USA* **44**, 98–104